Aromaticity of Square Planar N_4^{2-} in the M_2N_4 (M = Li, Na, K, Rb, or Cs) Species

Qian Shu Li* and Li Ping Cheng

School of Chemical Engineering and Materials Science, Beijing Institute of Technology, Beijing 100081, P. R. China

Received: October 30, 2002; In Final Form: February 22, 2003

A series of alkali metal−N_4^{2-} compounds M_2N_4 (M = Li, Na, K, Rb, or Cs) have been examined with ab initio and density functional theory (DFT) methods. To our knowledge, these compounds, except for the D_{4h} bipyramidal Li_2N_4, are first reported here. The bipyramidal structures with two metal cations above and below the N_4^{2-} plane are global minima for all five M_2N_4 systems. Kinetic analysis shows that the bipyramidal M_2N_4 species may exist or be characterized due to their significant isomerization or dissociation barriers (39.2−48.6 kcal/mol). Nucleus-independent chemical shifts (NICSs) criteria and the presence of six delocalized π-electrons (thus following the $4n + 2$ rule) confirmed that the square planar N_4^{2-} exhibits characteristics of aromaticity for these M_2N_4 species.

1. Introduction

Aromaticity, a concept generally associated with organic compounds, results in exceptional geometric, energetic, and magnetic properties.[1] It was initially bestowed on benzene and related compounds. Today, the proliferation of "types" of aromaticity goes far beyond the conventional confines and has been extended to include heterosystems,[2−4] inorganic molecules,[5,6] and transition metal oxides.[7] Recently, Li et al.[8,9] have investigated MAl_4^- (M = Li, Na, or Cu), gaseous $NaGa_4^-$, and $NaIn_4^-$. They reported evidences of aromaticity for these purely metallic systems, and thus, their findings expand the aromaticity concept into the arena of all-metal species. Later, they further extended the all-metal aromatic idea from Al_4^{2-} into a series of heteroclusters,[10] XAl_3^- (X = Si, Ge, Sn, and Pb). As Zandwijk et al.[11] reported, the isolated N_4^{2-} dianion has a minimum possessing a perfect square planar structure and six delocalized π-electrons, thus conforming to the $(4n + 2)$ rule for aromaticity. In the present work we first study structures and stabilities of a series of alkali metal−N_4^{2-} compounds M_2N_4 (M = Li, Na, K, Rb, or Cs) with the MP2 and B3LYP methods and then confirm the N_4^{2-} ring in the M_2N_4 species exhibits characteristics of aromaticity. Conventionally, aromaticity[12,13] is often discussed in terms of various criteria such as geometric (bond length equalization),[14,15] energetic (resonance and aromatic stabilization energies (ASEs)),[16,17] and magnetic (H^1 NMR chemical shifts, magnetic susceptibility anisotropies and their exaltations, and nucleus-independent chemical shifts (NICSs)) properties.[1−2,16,18−19] In this study we use the nucleus-independent chemical shift criteria and the presence of the $(4n + 2)$ π-electrons (thus following the $4n + 2$ rule) to confirm the aromaticity of N_4^{2-} in the M_2N_4 species.

2. Computational Methods

All calculations were performed using the Gaussian 98 program package.[20] We initially optimized geometries and calculated the harmonic vibrational frequencies of N_4^{2-}, Li_2N_4, Na_2N_4, and K_2N_4 at the B3LYP/6-311+G* level of theory, where B3LYP is the DFT method using Becke's three-parameter nonlocal functional[21] with the nonlocal correlation of Lee, Yang, and Parr[22] and 6-311+G* is the split-valence triple-ζ plus polarization basis set augmented with diffuse functions.[23] Then, the geometries were refined and the vibrational frequencies were calculated at the level of second-order Møller−Plesset perturbation theory (MP2)[24] with the 6-311+G* basis set. For N_4^{2-}, a square planar minimum was identified at the B3LYP/6-311+G* and MP2/6-311+G* levels of theory. We further studied it using the coupled cluster method [CCSD (T)][25] with the 6-311+G* basis set and found that it is a local minimum indeed, in agreement with the results obtained by Zandwijk et al.[11] With respect to K_2N_4, at the MP2 level, we calculated its vibrational frequencies with the 6-31+G* basis set using geometries optimized at the same level. The Rb_2N_4 and Cs_2N_4 model systems were optimized at the B3LYP and MP2 levels of theory, where the 6-311+G* basis set was used for nitrogen and the relativistic effective core potential with the LANL2DZ basis set was used for the two heavier metals Rb ($Z = 37$) and Cs ($Z = 55$).[26,27] Stationary points were characterized as minima without any imaginary vibrational frequency and a first-order saddle point with only one imaginary vibrational frequency. For transition states, the minimum energy pathways connecting the reactants and products were confirmed using the intrinsic reaction coordinate (IRC) method with the Gonzalez−Schlegel second-order algorithm.[28,29] Final energies were refined at the CCSD(T)/6-311+G*//B3LYP/6-311+G* + ZPE (B3LYP/6-311+G*) level of theory.

NICSs for N_4^{2-} were calculated with the GIAO-HF/6-311+G*//MP2/6-311+G* method. NICSs for Li_2N_4, Na_2N_4, and K_2N_4 were computed at GIAO-HF/6-311+G* on the B3LYP/6-311+G* geometries.[14,30] NICSs for Rb_2N_4 and Cs_2N_4 were evaluated by using the GIAO-HF//B3LYP method, where the 6-311+G* basis set was used for nitrogen and the LANL2DZ basis set was used for Rb and Cs. MOs of N_4^{2-}, Li_2N_4, Na_2N_4, and K_2N_4 were calculated at the RHF/6-311+G* level of theory. MOs of Rb_2N_4 and Cs_2N_4 were calculated at the RHF level of theory, where the 6-311+G* basis set was used for nitrogen and the LANL2DZ basis set was used for Rb and Cs. Since MOs of all similar structural M_2N_4 species are almost identical,

* Corresponding author. Telephone: 86-10-68912665. Fax: +86-10-68912665. E-mail: qsli@bit.edu.cn.

10.1021/jp027350n CCC: $25.00
Published on Web 03/28/2003

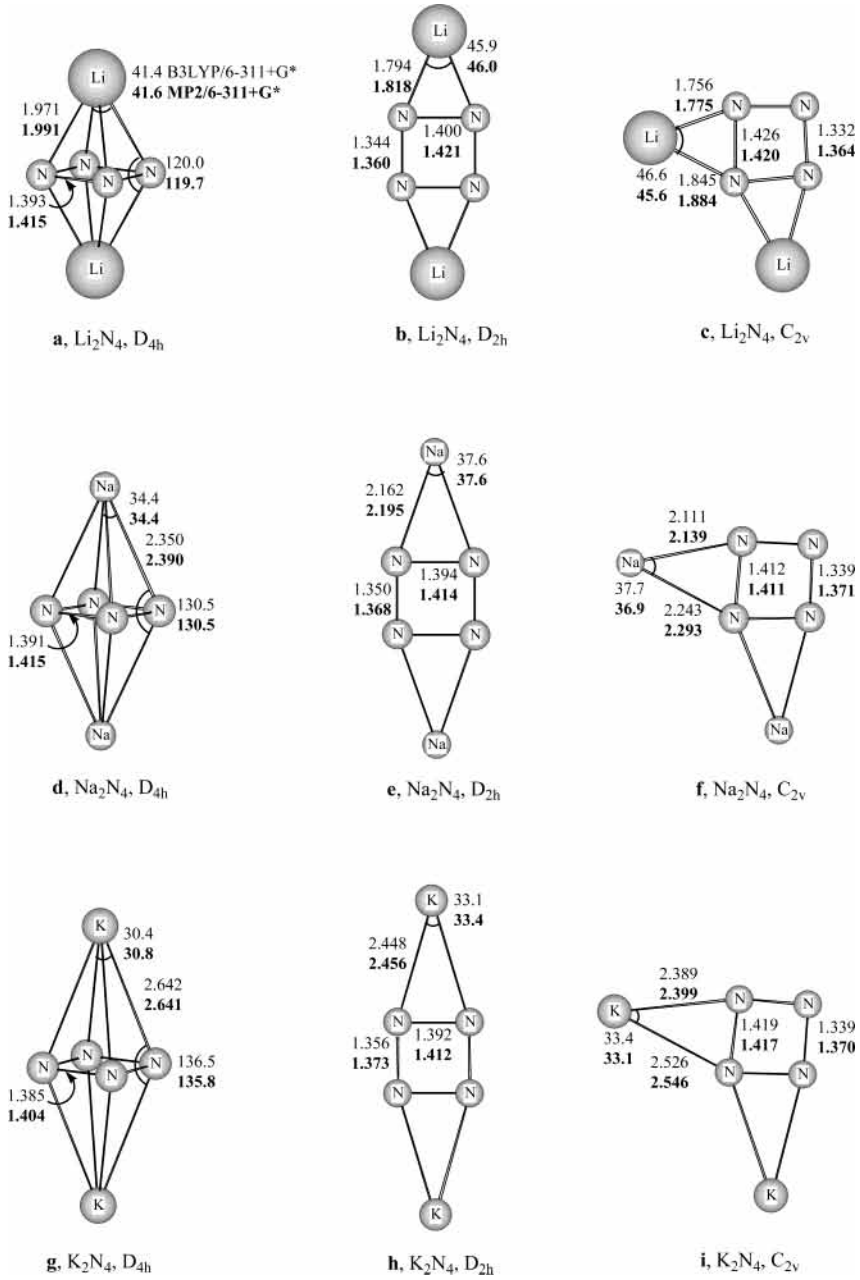

Figure 1. Optimized geometries (bond lengths in Å; bond angles in deg) for Li_2N_4 (**a**−**c**), Na_2N_4 (**d**−**f**), and K_2N_4 (**g**−**i**) species at the B3LYP/6-311+G* and MP2/6-311+G* (bold font) levels of theory.

herein we only display three series of MOs of Li_2N_4. All MO diagrams were made by using the MOLDEN 3.7 program.[31]

The natural bond orbital (NBO)[32,33] analysis is also performed to provide insight into the bonding nature and aromaticity of these species.

3. Results and Discussion

The optimized structures for five M_2N_4 systems and the N_4^{2-} dianion are illustrated in Figures 1 and 2. The total energies, zero-point energies (ZPE), relative energies (with zero-point vibrational energy corrections), and number of imaginary frequencies are tabulated in Table 1.

3.1. Structures and Stabilities of the M_2N_4 Species. *3.1.1. Geometric Structures and Energies of the M_2N_4 Species.* We performed ab initio calculations on a wide variety of structures and found that the bipyramidal structures with the two metal cations above and below the N_4^{2-} plane (Figures 1 and 2) are the global minima for all five M_2N_4 systems. All the M_2N_4 systems were also located in two planar structures containing the N_4^{2-} ring, that is, the D_{2h} planar and the C_{2v} planar structures (Figures 1 and 2). For Li_2N_4, the D_{4h} bipyramidal (Figure 1**a**), the D_{2h} planar (Figure 1**b**), and the C_{2v} planar (Figure 1**c**) structures are all local minima on the potential energy surfaces at the two used levels of theory (Table 1). The bipyramidal structure of Li_2N_4 had been previously studied by Zandwijk et al.[11] at the RHF/3-21G and RHF/6-31G* levels of theory. In the present study we calculated it at the B3LYP and MP2 levels of theory with the larger 6-311+G* basis set. For Li_2N_4, the global minimum D_{4h} bipyramid was found to be lower in energy than the D_{2h} planar structure and the C_{2v} planar structure by 13.3 and 19.6 kcal/mol at the B3LYP/6-311+G* level of theory, respectively. The corresponding values at the MP2/6-311+G* level are 15.4 and 23.0 kcal/mol, respectively. For Na_2N_4, the D_{2h} planar structure (Figure 1**e**) was found to be a local minimum 10.4 kcal/mol higher in energy than the D_{4h} bipyramid (Figure 1**d**) at the B3LYP/6-311+G* level of theory, but it is

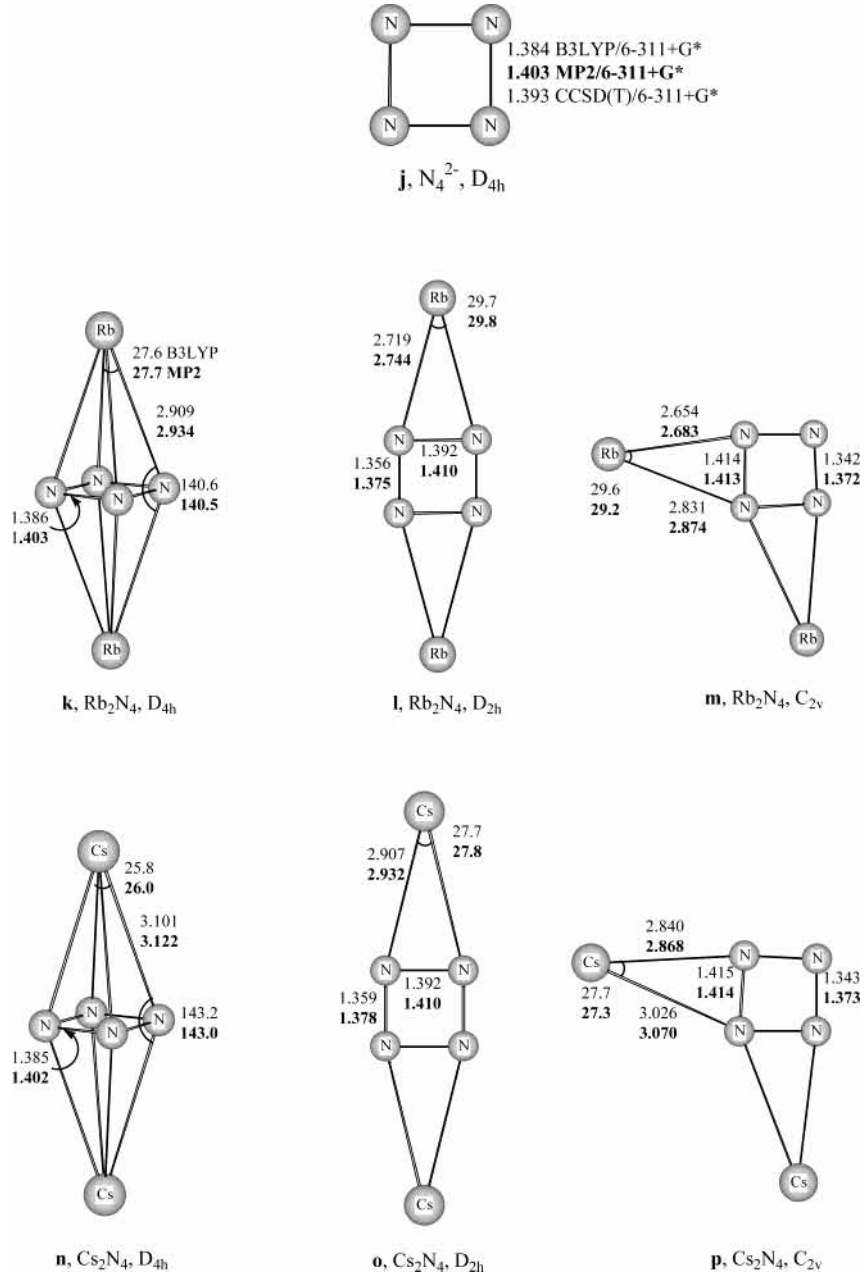

Figure 2. Optimized geometries (bond lengths in Å; bond angles in deg) for N_4^{2-} (**j**), Rb_2N_4 (**k**−**m**), Cs_2N_4 (**n**−**p**), Li_2N_4 (**q**), and K_2N_4 (**r**) at the B3LYP (CCSD (T) for N_4^{2-}) and MP2 (bold font) levels of theory.

TABLE 1: Total Energies (*E*),[a] Zero-Point Energies (ZPE),[b] and Relative Energies (RE)[c] for M_2N_4 Species

		B3LYP//6-311+G*			MP2//6-311+G*					B3LYP[e]			MP2[c]		
species		*E*[a]	ZPE[b]	RE[c]	*E*[a]	ZPE[b]	RE[c]	species		*E*[a]	ZPE[b]	RE[c]	*E*[a]	ZPE[b]	RE[c]
Li_2N_4	**a**	−234.0826	12.6 (0)	0.0	−233.4256	12.3 (0)	0.0	Rb_2N_4	**k**	−266.7294	10.3 (0)	0.0	−265.6489	10.2 (0)	0.0
	b	−234.0613	12.5 (0)	13.3	−233.4010	12.3 (0)	15.4		**l**	−266.7113	10.1 (1)	11.2	−265.6267	10.2 (0)	13.9
	c	−234.0509	12.3 (0)	19.6	−233.3886	12.1 (0)	23.0		**m**	−266.6994	9.9 (1)	18.4	−265.6124	9.9 (1)	22.6
Na_2N_4	**d**	−543.5961	10.9 (0)	0.0	−542.1877	10.6 (0)	0.0	Cs_2N_4	**n**	−258.7576	10.2 (0)	0.0	−257.6987	10.2 (0)	0.0
	e	−543.5795	10.9 (0)	10.4	−542.1682	10.7 (1)	12.3		**o**	−258.7387	10.0 (1)	11.7	−257.6748	10.0 (0)	14.8
	f	−543.5675	10.7 (1)	17.7	−542.1545	10.5 (1)	20.7		**p**	−258.7268	9.7 (1)	18.8	−257.6607	9.8 (1)	23.4
K_2N_4[d]	**g**	−1418.8962	10.8 (0)	0.0	−1416.7238	10.6(0)	0.0								
	h	−1418.8745	10.6 (0)	13.4	−1416.6961	10.6(0)	17.4								
	i	−1418.8633	10.5 (0)	20.3	−1416.6817	10.4 (0)	26.2								

[a] Total energies in Hartree. [b] Zero-point energies in kcal/mol. The integers in parentheses are the number of imaginary frequencies (NIMAG). [c] The relative energies with ZPE corrections in kcal/mol. [d] The listed total energies, ZPE, and relative energies for K_2N_4 at the B3LYP/6-311+G* and MP2/6-31+G* levels of theory. [e] The 6-311+G* basis set was used for nitrogen, and the LANL2DZ basis set was used for Rb and Cs.

a first-order saddle point 12.3 kcal/mol higher in energy at the MP2/6-311+G* level of theory. The C_{2v} planar structure (Figure 1**f**) is a first-order saddle point 17.7 and 20.7 kcal/mol higher in energy than the D_{4h} bipyramid (Figure 1**d**) at the B3LYP/6-311+G* and MP2/6-311+G* levels of theory, respectively. Regarding K_2N_4, the D_{2h} planar structure (Figure 1**h**) was found

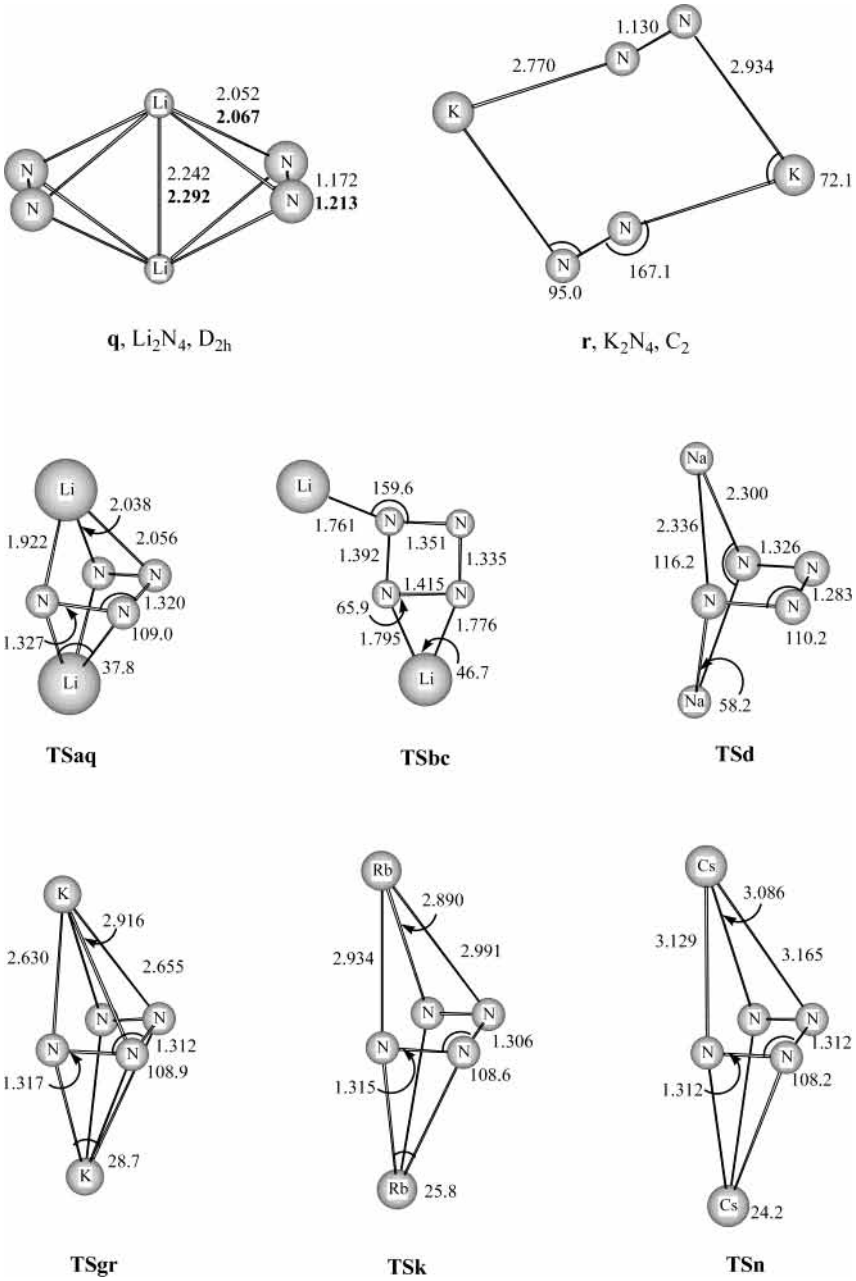

q, Li_2N_4, D_{2h} **r**, K_2N_4, C_2

TSaq **TSbc** **TSd**

TSgr **TSk** **TSn**

Figure 3. Six transition states (bond lengths in Å; bond angles in deg) for decomposition and isomerization reactions for some M_2N_4 species.

TABLE 2: Zero-Point Corrected B3LYP Energies (kcal/mol) for Hypothetical $M_2N_4 \rightarrow 2M^+ + N_4^{2-}$ Reactions

Li_2N_4			Na_2N_4			K_2N_4			Rb_2N_4			Cs_2N_4		
a	**b**	**c**	**d**	**e**	**f**	**g**	**h**	**i**	**k**	**l**	**m**	**n**	**o**	**p**
455.1	441.8	435.5	399.1	388.7	381.4	369.8	356.4	349.4	335.0	323.9	316.6	320.6	308.9	301.7

to be a local minimum 13.4 and 17.4 kcal/mol higher in energy than its bipyramidal structure (Figure 1**g**) at the B3LYP/6-311+G* and MP2/6-31+G* levels of theory, respectively. The C_{2v} planar structure (Figure 1**i**) is also a local minimum at both B3LYP/6-311+G* and MP2/6-31+G* levels of theory. It is energetically higher than the bipyramidal structure by 20.3 and 26.2 kcal/mol at the above two levels, respectively. Regarding Rb_2N_4 and Cs_2N_4 systems, the D_{2h} planar structures (Figure 2**l** and 2**o**) are all first-order saddle points at the B3LYP level of theory, but they are all local minima at the MP2 level. The C_{2v} planar structures (Figure 2**m** and 2**p**) are all first-order saddle points at the two levels of theory. At the MP2 level the global minimum D_{4h} bipyramidal structure (Figure 2**k** and 2**n**) is more stable than the D_{2h} planar structure by 13.9 and 14.8 kcal/mol for Rb_2N_4 and Cs_2N_4, respectively. The C_{2v} planar structures of Rb_2N_4 and Cs_2N_4 are higher in energy than their global minimum by 22.6 and 23.4 kcal/mol at the MP2 level of theory, respectively.

Besides the above-mentioned M_2N_4 structures, we have located an edge-sharing bitetrahedral structure (Figure 2**q**) and a closed-chain structure (Figure 2**r**) for Li_2N_4 and K_2N_4, respectively. Although the two conformers have the general formula M_2N_4, they are not containing an N_4^{2-} ring. So, less attention will be paid to them in the present study.

As shown in Figures 1 and 2, for each set of the similar structural M_2N_4 species, the lighter the alkali metal is, the shorter the M−N distances are. Regarding the N−N distances in the M_2N_4 compounds, for the bipyramidal structures, all N−N

TABLE 3: Total Energies [*E* (hartrees)], Zero-Point Energies [ZPE (kcal/mol)], and Lowest Vibrational Frequencies [υ_1 (cm^{-1})] for the Transition States

isomer	*E*	B3LYP/ 6-311+G* ZPE	υ_1	CCSD (T)/6-311+G*// B3LYP/6-311+G*
TSaq (C_2)	−233.9978	9.9	784*i*	−233.3635
TSbc (C_1)	−234.0431	11.9	143*i*	−233.4018
TSd (C_2)	−543.5269	8.7	714*i*	−542.1392
TSgr (C_2)	−1418.8165	8.5	787*i*	−1417.1225
TSk (C_2)	−266.6585	8.2	786*i*	−265.5927
TSn (C_2)	−258.6859	8.1	809*i*	−257.6409

TABLE 4: Energy Differences (kcal/mol) of Transition States Relative to M_2N_4 Isomers (Including ZPE Corrections at the B3LYP/6-311+G* Level)

isomer	B3LYP/6-311+G*	CCSD (T)/6-311+G*// B3LYP/6-311+G*
a (D_{4h})	0.0	0.0
TSaq (C_2)	50.5	48.6
b (D_{2h})	0.0	0.0
TSbc (C_1)	10.8	10.5
c (C_{2v})	0.0	0.0
TSbc (C_1)	4.5	4.5
d (D_{4h})	0.0	0.0
TSd (C_2)	41.2	39.2
g (D_{4h})	0.0	0.0
TSgr (C_2)	47.7	47.0
k (D_{4h})	0.0	0.0
TSk (C_2)	42.4	44.9
n (D_{4h})	0.0	0.0
TSn (C_2)	42.9	46.0

distances are slightly longer than that in the bare N_4^{2-} ring (Figure 2**j**), and the amount of lengthening gives a decreasing trend from Li to heavier atoms. This indicates that the lighter the metal is, the more the M^+ affects the N_4^{2-} ring. For the D_{2h} and C_{2v} planar structures, in all methods, the presence of the cation on the side of the ring induces alternating N−N distances. In addition, like the case of the isolated N_4^{2-} dianion, all N−N−N bond angles are about 90° in the N_4^{2-} rings of the M_2N_4 species. Mulliken charge analysis shows that all positive charges locate on the alkali metal atoms and all negative charges on the nitrogen atoms for all M_2N_4 species. In terms of NBO analysis, the calculated NN Wiberg bond indices (WBIs) range from 1.2 to 1.4, indicating delocalization. That all WBIs of metal−nitrogen are close to zero supports that the role of the M^+ is to stabilize the electronically unstable N_4^{2-} dianion, and the M^+ cations have relatively minor effects on the electronic structure of the dianion. Therefore, we predict that electrostatic interaction is dominant in the M_2N_4 compounds.

3.1.2. Stabilities of the M_2N_4 Systems. The zero-point corrected B3LYP energies for hypothetical $M_2N_4 \rightarrow 2M^+ + N_4^{2-}$ reactions are given in Table 2. All reactions are endothermic, indicating that the M_2N_4 species are stable toward decomposition. Furthermore, the lighter the alkali metal is, the more energy the reaction needs. Therefore, the Li_2N_4 system is the most stable one among these five M_2N_4 systems.

We have investigated the isomerization and decomposition reactions for some M_2N_4 species by using the B3LYP method. The optimized structures for six transition states are shown in Figure 3. Their total energies, zero-point energies (ZPEs), and lowest vibrational frequencies are listed in Table 3. The energy differences between the minima and their corresponding transition states are tabulated in Table 4.

As shown in Figure 3, a transition structure **TSaq** (C_2) was located connecting the bipyramidal Li_2N_4 **(a)** to the edge-sharing bitetrahedral Li_2N_4 **(q)**. The barrier going from **a** to **q** is 48.6 kcal/mol at the CCSD (T)/6-311+G*//B3LYP/6-311+G* + ZPE (B3LYP/6-311+G*) level of theory. Similarly, we located a transition structure **TSgr** (C_2) connecting the bipyramidal K_2N_4 **(g)** to the closed chain K_2N_4 **(r)**. The corresponding barrier from **g** to **r** is 47.0 kcal/mol evaluated at the CCSD (T) level of theory. Therefore, the bipyramidal Li_2N_4 and K_2N_4 possess significant kinetic stability toward isomerization. The possible isomerization from the Li_2N_4 **(b)** to the Li_2N_4 **(c)** was also studied. The two conformers interconvert through a transition structure **TSbc** (seen in Figure 3). Conformer **b** converts to **c** with a barrier of 10.5 kcal/mol, and conformer **c** converts to **b** with a barrier of 4.5 kcal/mol. The low barrier heights of the isomerization reaction suggest that the Li_2N_4 **(b)** and the Li_2N_4 **(c)** are kinetically unstable.

TABLE 5: Calculated NICS Values with the GIAO-HF/ 6-311+G*//MP2/6-311+G* Method for N_4^{2-}, the GIAO-HF/ 6-311+G*//B3LYP/6-311+G* Method for Li_2N_4, Na_2N_4, and K_2N_4 Species and the GIAO-HF//B3LYP Method for Rb_2N_4 and Cs_2N_4 Species

species		NICS(0.0)	NICS(0.5)	NICS(1.0)	NICS(1.5)
Li_2N_4	**a**	−0.81	−10.67	−14.65	−44.81
	b	3.03	−3.70	−6.42	−4.36
	c	1.48	−4.34	−6.38	−4.21
Na_2N_4	**d**	6.09	−2.44	−6.52	−17.04
	e	2.42	−3.09	−5.31	−3.61
	f	2.59	−2.70	−4.83	−3.26
K_2N_4	**g**	1.63	−7.60	−9.93	−16.08
	h	3.16	−2.82	−5.37	−3.74
	i	2.51	−2.76	−4.95	−3.43
N_4^{2-}	**j**	3.98	−1. 60	−4.09	−2.93
Rb_2N_4	**k**	3.69	−4.88	−6.85	−8.08
	l	2.83	−2.65	−4.89	−3.40
	m	2.62	−2.35	−4.40	−3.08
Cs_2N_4	**n**	2.88	−5.39	−6.61	−6.21
	o	3.51	−2.25	−4.74	−3.34
	p	3.16	−2.04	−4.31	−3.06

The decomposition mechanisms of the bipyramidal Na_2N_4, Rb_2N_4, and Cs_2N_4 are investigated in our present work. As shown in Figure 3, three transition structures **TSd**, **TSk**, and **TSn** with C_2 symmetry were located. Starting from **TSd**, **TSk,** and **TSn**, the IRC calculations directly lead to dissociation into Na_2, Rb_2, as well as Cs_2 and two N_2 molecules, respectively. The barrier heights for the decomposition reactions **d** → **TSd** → $Na_2 + 2N_2$, **k** → **TSk** → $Rb_2 + 2N_2$, and **n** → **TSn** → $Cs_2 + 2N_2$ are predicted to be 39.2, 44.9, and 46.0 kcal/mol at the CCSD (T) level of theory, respectively, indicating the high kinetic stability.

Our kinetic analysis shows that all bipyramidal M_2N_4 structures are likely to be stable and to be observed experimentally.

3.2. Aromaticity of N_4^{2-} in the M_2N_4 Species. *3.2.1. Nucleus-Independent Chemical Shift (NICS).* NICS, proposed by Schleyer and co-workers,[2,34] is an efficient and simple criterion in probing aromaticity, which is based on the negative of the magnetic shielding computed, for example, at or above the geometrical centers of rings or clusters. Systems with (significant) negative NICS values are aromatic, and systems with strongly positive NICS values are antiaromatic. Nonaromatic cyclic systems should therefore have NICS values around zero. The more negative the NICS, the more aromatic the system is.[2,30] In this study we first calculated NICS(0.0) and NICS(1.0), by placing a ghost atom at and above (by 1.0 Å) the geometric centers of the nitrogen four-membered ring, respectively, but we found results obtained from the two places are greatly discrepant. As tabulated in Table 5, on the basis of the calculated NICS(0.0) values, most M_2N_4 species are nonaromatic or weakly antiaromatic according to the yardstick of a 50% value

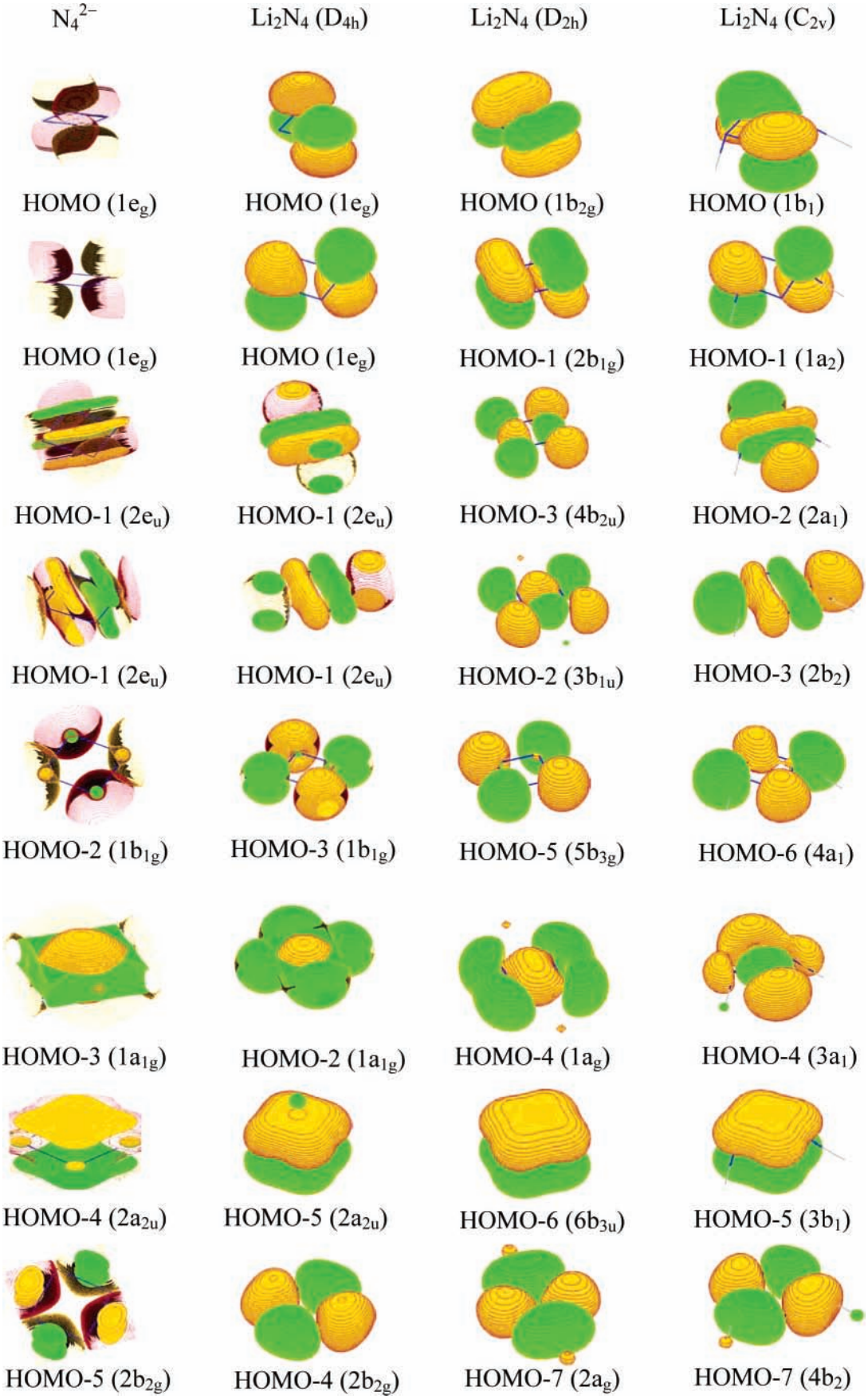

Figure 4. Molecular orbital contour figures of the bare N_4^{2-}, D_{4h} bipyramidal Li_2N_4, D_{2h} planar Li_2N_4, and C_{2v} planar Li_2N_4, showing the HOMO down to the fifth valence molecular orbital (HOMO-5) for N_4^{2-} and Li_2N_4 (D_{4h}) as well as the HOMO down to the seventh valence molecular orbital (HOMO-7) for Li_2N_4 (D_{2h}) and Li_2N_4 (C_{2v}).

of benzene (−7.8 at $z = 0.0$ Å).[18] However, according to the calculated NICS(1.0) values, all M_2N_4 species are aromatic. To further analyze the aromaticity, we also calculated NICS(0.5) and NICS(1.5) values. The calculated results are also listed in Table 5. We found that the NICS(0.5) value is intermediate between that of NICS(0.0) and NICS(1.0) for all M_2N_4 species, but it tends to exhibit aromatic character. As tabulated in Table 5, the NICS(1.5) value is intermediate between that of NICS-(0.5) and NICS(1.0) for most D_{2h} planar and C_{2v} planar species. But NICS(1.5) values of −44.81, −17.04, and −16.08 for the bipyramidal Li_2N_4, Na_2N_4, and K_2N_4 are far larger than their NICS(0.0), NICS(0.5), and NICS(1.0) values, respectively. Furthermore, the shorter the distance between metal and nitrogen is, the more the NICS value increases. This phenomenon suggests that NICS(1.5) values are seriously influenced by the alkali metals. In addition, NICS(0.0) values in the ring plane are influenced by the local contributions of the N−N σ bonds and lone pairs.[2] Therefore, as Schleyer et al.[2] reported, NICS-(1.0) values are better suited for the interpretation of π-contributions and to answer the question whether the M_2N_4 species are really aromatic. As shown in Table 5, the absolute NICS(1.0) values for all M_2N_4 species are larger than that of the isolated N_4^{2-} dianion (−4.09). The introduction of counterions seems to result in an increase in aromaticity to some extent. For M_2N_4 systems with the same metal atoms, the NICS(1.0) criterion gives the following aromaticity order: the D_{4h} bipyramidal > the D_{2h} planar > the C_{2v} planar. NICS(1.0) values of M_2N_4 give a decreasing trend from Li to heavier atoms. This trend may be attributed to the distances between the M^+ cations and the N_4^{2-} ring. For each set of the similar structural M_2N_4 species, structural analysis indicates that the lighter the alkali metal is, the shorter the M−N distances are and the more the M^+ affects the N_4^{2-} ring. Furthermore, Mulliken charge and NBO analysis suggest that the electrostatic interaction is dominant in the M_2N_4 compounds. Therefore, the electrostatic interaction in Li_2N_4 compounds is stronger and the Li^+ cation may attract more electron density from the N_4^{2-} ring compared with other M^+ cations. Correspondingly, the absolute NICS(1.0) values are larger in Li_2N_4 system. NICS(1.0) values are appreciable in the bipyramidal Li_2N_4 (−14.65) and K_2N_4 (−9.93), comparable to the benzene value (−10.0 at $Z = 1.0$ Å).[18] NICS(1.0) values range from −4.31 to −6.85 for other M_2N_4 species, indicating a small degree of aromaticity.

It should be mentioned that the GIAO NICS (−4.09) seems to show that the N_4^{2-} dianion is not so aromatic. But considering it is a small-ring molecule, the NICS values based on the GIAO method may be greatly influenced by N−N σ-bonds and lone pairs, and we have dissected the NICS using the IGLO method.[35] However, the dissected NICS shows that the π-contribution is large (−23.0). The corresponding benzene value is −22.0. Although we cannot say N_4^{2-} is more aromatic than benzene (because small rings often give large NICSs), it is surely aromatic. We believe that a similar situation would happen for the N_4^{2-} rings in the M_2N_4 species; that is, they are aromatic.

3.2.2. Presence of (4n + 2) Number of π-Electrons. As shown in Figure 4, the two degenerate HOMOs ($1e_g$) of N_4^{2-} are nonbonding orbitals formed from the out-of-plane 2p orbitals, and they are π-bonding MOs. The two degenerate HOMO-1 orbitals ($2e_u$) are also nonbonding orbitals formed from the in-plane 2p orbitals. HOMO-2 ($1b_{1g}$), HOMO-3 ($1a_{1g}$), HOMO-4 ($2a_{2u}$), and HOMO-5 ($2b_{2g}$) are bonding orbitals. HOMO-2 ($1b_{1g}$) is mainly formed from 2s orbitals of N_4^{2-}. HOMO-3 ($1a_{1g}$) is formed from the in-plane 2p orbitals. HOMO-4 ($2a_{2u}$) is formed from the out-of-plane 2p orbitals, and it is a π-bonding MO. HOMO-5 ($2b_{2g}$) is also formed from the in-plane 2p orbitals. Altogether, there are three π-bonding MOs, HOMO (including two degenerate orbitals) and HOMO-4, in N_4^{2-}, involved six π-electrons and rendered aromaticity to this species. Certainly, the presence of the π-bonding MOs plays an important role in the stabilization of this multiply charged species. But the σ-bonding MOs composed of s-orbitals and (in-plane) p-orbitals also have effects. It is the perfect square planar structure's bonding nature in MOs that makes this species stable and resists all distortions from this conformation.

Figure 4 shows that the MOs of the N_4^{2-} dianion can be easily recognized in all M_2N_4 species even though the orders of some MOs are varied. They are only changed slightly by the presence of the counterions, showing the presence of six π-electrons in the N_4^{2-} ring and the electronic integrity of the aromatic dianion in the M_2N_4 species.

On the basis of the above analysis, we came to the conclusion that N_4^{2-} indeed exhibits characteristics of aromaticity for these M_2N_4 species.

4. Summary

We reported a series of alkali metal−N_4^{2-} compounds M_2N_4 (M = Li, Na, K, Rb, or Cs) and showed that their bonding can be viewed as two alkali metal cations interacting with a square planar N_4^{2-} dianion. To our knowledge, these compounds, except for the D_{4h} bipyramidal Li_2N_4, are first reported here. All the M_2N_4 systems were located in three structures containing the N_4^{2-} ring, that is, the D_{4h} bipyramidal, the D_{2h} planar, and the C_{2v} planar structures. Among them, the bipyramidal structures with two metal cations above and below the N_4^{2-} plane are the most energetically favored. Kinetic analysis shows that the bipyramidal M_2N_4 structures are likely to be stable and may exist or be characterized. The appreciable NICS(1.0) values and the presence of six π-electrons (thus following the $4n + 2$ rule) confirmed that the square planar N_4^{2-} indeed exhibits characteristics of aromaticity for these M_2N_4 species.

Acknowledgment. We thank Dr. Zhi-Xiang Wang for his help.

References and Notes

(1) Schleyer, P. v. R.; Jiao, H. *Pure Appl. Chem.* **1996**, *68*, 209.
(2) Schleyer, P. v. R.; Jiao, H.; Hommes, N. v. E.; Malkin V. G.; Malkina, O. L. *J. Am. Chem. Soc.* **1997**, *119*, 12669.
(3) Bird, C. W. *Tetrahedron* **1998**, *54*, 4641.
(4) Goldfuss, B.; Schleyer, P. v. R. *Organometallics* **1997**, *16*, 1543.
(5) King, R. B. *J. Chem. Inf. Comput. Sci.* **1992**, *32*, 42.
(6) Hirsch, A.; Chen, Z.; Jiao, H. *Angew. Chem., Int. Ed.* **2001**, *40*, 2834.
(7) King, R. B. *J. Chem. Inf. Comput. Sci.* **2001**, *41*, 517.
(8) Li, X.; Kuznetsov, A. E.; Zhang, H. F.; Boldyrev, A. I.; Wang, L. S. *Science* **2001**, *291*, 859.
(9) Kuznetsov, A. E.; Boldyrev, A. I.; Li, X.; Wang, L. S. *J. Am. Chem. Soc.* **2001**, *123*, 8825.
(10) Li, X.; Zhang, H. F.; Wang, L. S.; Kuznetsov, A. E.; Cannon, N. A.; Boldyrev, A. I. *Angew. Chem., Int. Ed.* **2001**, *40*, 1867.
(11) Zandwijk, G. v.; Janssen, R. A. J.; Buck, H. M. *J. Am. Chem. Soc.* **1990**, *112*, 4155.
(12) Cyrañski, M. K.; Krygowski, T. M.; Katritzky, A. R.; Schleyer, P. v. R. *J. Org. Chem.* **2002**, *67*, 1333.
(13) Krygowski, T. M.; Cyrañski, M. K.; Czarnocki, Z.; Häfelinger, G.; Katritzky, A. R. *Tetrahedron* **2000**, *56*, 1783.
(14) Eluvathingal, D. J.; Boggavarapu, K. *Inorg. Chem.* **1998**, *37*, 2110.
(15) Krygowski, T. M. *J. Chem. Inf. Comput. Sci.* **1993**, *33*, 70.
(16) Goldfuss, B.; Schleyer, P. v. R.; Hampel, F. *Organometallics* **1996**, *15*, 1755.
(17) Glukhovtsev, M. *J. Chem. Educ.* **1997**, *74*, 132.
(18) Willard, C.; Svein, S.; Charles, U. P. J. *J. Mol. Struct. (THEOCHEM)* **2001**, *549*, 1.

(19) Wolinski, K.; Hilton, J. F.; Pulay, P. Efficient Implenmentation of the Gange-Independent Atomic Orbital Method for NMR Chemical Shift Calculations. *J. Am. Chem. Soc*. **1990**, *112*, 8251.
(20) Frisch, M. J.; et al. *GAUSSIAN 98*, Revision A.9; Gaussian, Inc.: Pittsburgh, PA, 1998.
(21) Becke, A. D. *J. Chem. Phys.* **1993**, *98*, 1372.
(22) Lee, C.; Yang, W.; Parr, R. G. *Phys. Rev.* B **1988**, *37*, 785.
(23) Hehre, W. J.; Radom, L.; Schleyer, P. v. R.; Pople, J. A. *Ab initio Molecular Orbital Theory*; Wiley: New York, 1986.
(24) Møller, C.; Plesset, M. S. *Phys. Rev.* **1934**, *46*, 618.
(25) Cizek, J. *Adv. Chem. Phys.* **1969**, *14*, 35.
(26) Hay, P. J.; Wadt, W. R. *J. Chem. Phys.* **1985**, *82*, 270.
(27) Wadt, W. R.; Hay, P. J. *J. Chem. Phys.* **1985**, *82*, 284.
(28) Gonzalez, C.; Schlegel, H. B. *J. Chem. Phys.* **1989**, *90*, 2154.
(29) Gonzalez, C.; Schlegel, H. B. *J. Phys. Chem.* **1990**, *94*, 5523.
(30) Schleyer, P. v. R.; Najafian, K.; Kiran, B.; Jiao, H. *J. Org. Chem.* **2000**, *65*, 426.
(31) Schaftenaar, G. *MOLDEN3.7*; CAOS/CAMM Center: The Netherlands, 1998.
(32) Carpenter, J. E.; Weinhold, F. *J. Mol. Struct. (THEOCHEM)* **1988**, *169*, 41.
(33) Reed, A. E.; Weinstock, R. B.; Weinhold, F. *J. Chem. Phys.* **1985**, *83*, 735.
(34) Schleyer, P. v. R.; Maerker, C.; Dransfeld, A.; Jiao. H.; Hommes, N. v. E. *J. Am. Chem. Soc.* **1996**, *118*, 6317.
(35) (a) Malkin. V. G.; Malkin, O. L.; Eriksson, L. A.; Salahub, D. R. In *Modern Density Functional Theory*; Seminario. J. M., Politzer, P., Eds.; Elsevier: Amsterdam, 1995; p 273. (b) Malkin, V. G.; Malkin, O. L.; Eriksson, L. A.; Salahub, D. R. *J. Am. Chem. Soc*. **1994**, *116*, 5898.